Screening CO_2 storage potential of petroleum reservoirs on the Norwegian Continental Shelf

Alexey Khrulenko [a]*, Trine Mykkeltvedt [a], Sarah E. Gasda [a,b]
[a] *NORCE Norwegian Research Center, Nygårdsgaten 112, 5008 Bergen, Norway*
[b] *University of Bergen, Allégaten 41, 5007 Bergen, Norway*

Abstract

This study aims to assess the CO_2 storage potential of petroleum fields on the Norwegian Continental Shelf (NCS) using publicly available well and reservoir data. A set of indicators is proposed to infer CO_2 storage capacity, injectivity, remaining production time, and other relevant parameters. The original and enriched data, along with the derived indicators, have been compiled into a database covering 134 Norwegian fields. The total storage capacity indicator is estimated at 18 Gt, with 64% attributed to the ten largest fields and 69% to gas production.

The presented approach is simple, transparent, reproducible, and relies solely on open data. It enables screening, highlighting knowledge gaps and key areas for further detailed studies, and consistently comparing candidate reservoirs. The proposed methodology is illustrated by two case studies.

The findings and data from this study have broader applications, such as hydrogen storage, demonstrating significant potential for further reuse of data from petroleum reservoirs. The data and codes are openly accessible at *https://github.com/cssr-tools/SubCSeT*, and a web application for visualization and screening is available at *https://subcset-35e143428f88.herokuapp.com*.

Keywords: CO_2 storage; screening; ranking; petroleum fields; Norway; Norwegian Continental Shelf

1. Introduction

To fulfill Europe's CO_2 abatement objectives in the coming years, substantial new initiatives are needed to secure sufficient and economical CO_2 storage capacity. Repurposing depleted petroleum fields can play a key role in achieving this goal due to their ample pore space, good flowing properties, and secure caprocks [18]. These fields, having securely contained hydrocarbons for thousands of years, may become ideal candidates for CO_2 storage.

To date, around 130 petroleum fields on the Norwegian Continental Shelf (NCS) have been approved for production, with 55% of the resources produced by December 31, 2023 ([1], figure 4.3). This implies large, depleted pore volumes that can be reused. Given the increasing demand for CO_2 storage and presence of abandoned or soon-to-be-abandoned fields near existing infrastructure, their potential is likely to be utilized in the future. As in the case of natural gas storage in the USA, where depleted petroleum reservoirs account for 78.2% of total storage capacity, compared to 14.8% in aquifers and 7% in caverns [2].

Despite growing interest in CO_2 storage in saline aquifers on the NCS, relatively few studies have considered pure CO_2 storage (i.e., without an enhanced oil recovery component) in petroleum fields. To our knowledge, the most comprehensive account was given in the CO_2 Storage Atlas [15] for the Norwegian North Sea, which estimated storage capacity in 12 fields abandoned by the end of 2013 at 3 Gt. Additionally, 4 Gt and 6 Gt were estimated to become

* Corresponding author. Tel.: +47 51 87 52 74, *E-mail address:* alkh@norceresearch.no

available in 2030 and 2050, respectively, totaling 10 Gt by 2050. Troll, the largest Norwegian gas field, and its aquifer were estimated to accommodate 14 Gt after 2050. For comparison, the total storage capacity (i.e., including aquifers and petroleum fields) was estimated at approximately 86 Gt. Unfortunately, no further estimates were provided for individual fields.

Many works have been published on assessment of CO_2 storage potential in other regions, saline aquifers, and various screening techniques (see, for instance, the studies by Ramirez et al. [9], Bachu [16], Bergmo et al. [17]). The work by Ramirez et al. [9], which we consider the most relevant for our study, presented a comprehensive methodology covering both saline aquifers and petroleum reservoirs in the Netherlands, discussing how different types of data can be qualitatively and quantitatively utilized to screen and rank reservoirs by their potential storage capacity, storage costs, and effort needed to manage risk. Notably, the authors proposed treating data uncertainty as a separate screening criterion, an idea that was later implemented in the study by Bergmo et al. [17].

The current study presents an approach for screening petroleum fields on the NCS for CO_2 storage, based mainly on well and reservoir data made publicly available by the Norwegian Offshore Directorate (NOD) [3], [4]. The main idea of our approach is to leverage existing knowledge about petroleum fields to assess their suitability for CO_2 storage. The second part presents workflows employed for data collection, processing and enrichment, and derivation of various metrics (indicators) relevant for CO_2 storage. These metrics aim to assess the suitability of the given reservoir for CO_2 storage based on its development history and other available background data. For instance, an indicator based on produced volumes is used to characterize storage capacity and historical production rates are used to track injectivity and reservoir flow properties. The third part demonstrates the methodology through examples. The paper concludes with a discussion of the applicability and limitations of the proposed approach and suggests ways forward.

The described screening approach is implemented in a web application openly available at *https://subcset-35e143428f88.herokuapp.com*. The data and codes are available at *https://github.com/cssr-tools/SubCSeT*.

2. Methodology

2.1. Data sources

The main idea of our approach is to utilize publicly available reservoir data to derive certain *indicators* relevant to CO_2 storage. A brief overview of data sources, data flows and resulting indicators is presented in Fig. 1. The main data sources used in our study are:

- The FactPages of the Norwegian Offshore Directorate [3]:
    - field descriptions: main producing groups and formations, coordinates, lithology,
    - field in-place and recoverable volumes,
    - field production profiles,
    - wellbore data: final depth (SSTVD), temperature, type, completion date.
- DISKOS (public portal) [4]:
    - field production and injection rates,
    - well production and injection rates.
- literature [7]: initial pressures, temperatures, depths.

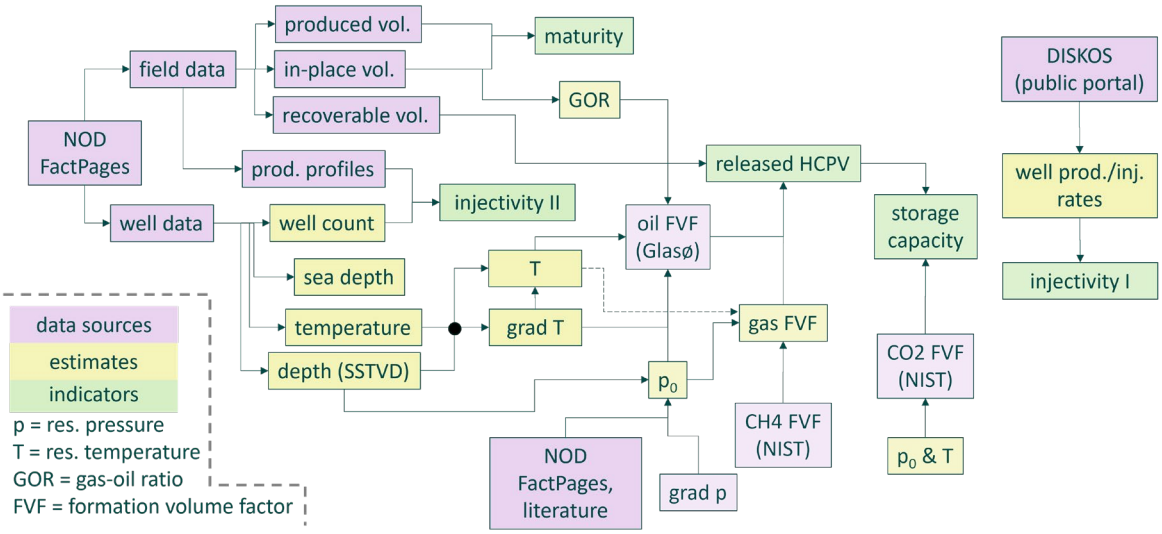

Fig. 1. Simplified scheme of data sources, data flows and derived indicators

2.2. Indicators

The resulting database covers 134 Norwegian fields that have been ever approved for production. The data retrieval, processing, feature engineering workflows, data references, and many other details are documented in a Jupyter Notebook named *main.ipynb* in the GitHub repository [5].

The **reservoir depth** for each field is estimated as the average subsea true vertical depth of its development wells and adjusted where better data are available. Development (i.e., production, injection, and observation) wells are counted, with laterals considered as separate wells.

The **initial reservoir temperature** is estimated from temperatures and depths reported for exploration wells. Despite the abundant data, applying these estimates directly to all individual reservoirs is challenging due to missing data, outliers, and verification difficulties. Therefore, linear regression (Fig. 2) is used to estimate the temperature gradient and intercept from all data points, yielding the relationship $T(z)=32.3z+7.9$ °C, where z represents subsea true vertical depth (km). For comparison, the study [6] reported a similar relationship $T(z)=31.7z+3.4$ °C for the Sleipner CO_2 storage complex. The derived relationship is then used to calculate the reservoir temperature for individual fields from the reservoir depth. A few data points are updated with more accurate estimates found in the literature and the FactPages [3]; a complete list of sources is maintained in the project repository [5]. However, the accuracy could be further improved by employing more advanced data mining techniques, which is an obvious way forward.

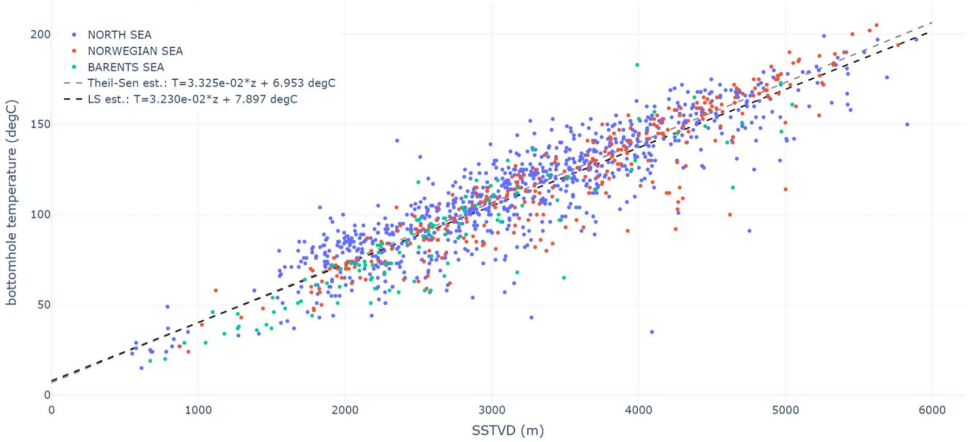

Fig. 2. Illustration of the regression of temperature data. Colors represent different NCS regions. Dashed lines depict the use of different regression methods: Theil-Sen and ordinary least squares

The **initial reservoir pressure** (**p0**), in the first approximation, is assumed to be hydrostatic, with a gradient of 101.8 bar/km (or 1.038 g/cm^3 in the drilling mud density equivalent). This assumption holds for most relatively shallow reservoirs (up to 2 km). However, the hydrostatic pressure gradient represents the lower boundary; in deeper reservoirs, it may reach up to twice this value. Therefore, significant effort has been made to correct pressure estimates and minimize uncertainty propagation to pressure-dependent parameters by using measurements from discovery and appraisal well reports [3], as well as regional pressure trends from [7] (e.g., for Brent reservoirs and the Greater Ekofisk area). For more details, refer to [5]. An additional property (**p0 checked**) is introduced to indicate whether the initial pressure has been verified. The ratio of initial pressure to depth yields the **initial pressure gradient**, which, if the field is overpressured, may suggest a limited connected aquifer volume.

The **initial gas-oil ratio** (GOR) is estimated as the ratio of the associated gas volume to the Stock Tank Oil Initially in Place (STOIIP) and is corrected where possible. The gas Formation Volume Factor (FVF) is estimated for methane at the initial pressure and temperature using the NIST database [8]. Although the dry gas assumption may yield relatively large errors for wet gas reservoirs, we believe these errors remain consistent with the quality of the input data and are acceptable for the purposes of this study. Similar reasoning applies to the use of the Glasø correlation to estimate the oil FVF.

The derived parameters allow for estimating the initial hydrocarbon pore volume (HCPV) and its share released during production. By multiplying this released volume by the CO_2 density at initial pressure and temperature (calculated from the NIST data tables [8]), we obtain a **CO_2 storage capacity indicator** (similar to the metric proposed in [9]). The physical meaning of the indicator is the amount of CO_2 that can be stored in the reservoir at the initial pressure in the absence of 1) compaction, 2) CO_2 dissolution in oil and brine, and 3) water volumes injected for pressure support (mainly due to availability and verification difficulties). The storage capacity indicator divided by the well count yields the **storage capacity per legacy well**, which can be used to factor in well leakage risk if there are such concerns.

Injectivity indicators aim to assess the reservoir's flow properties based on its production history, as higher historical production and injection well rates are likely to be associated with better flow properties. Water and gas injection rates could serve as a good benchmark; however, they are unavailable for fields produced by depletion. Moreover, gas injection is often employed to utilize excess gas volumes produced in oil fields. On the other hand, while production rates are readily available, consistent comparison between oil and gas producing wells is challenging due to differences in pressure, volume, temperature (PVT) properties, and production constraints. In our study, this challenge is addressed by converting production volumes to pseudo-reservoir conditions, utilizing calculated

formation volume factors at initial reservoir pressure and gas-oil ratio. I.e., this approach allows tracking how quickly the reservoir pore volume was vacated during production. Two injectivity indicators are calculated from:

1. well fluid production rates and operating time from the DISKOS database [4]
2. field production and well count data from the NOD FactPages [3] for the peak production year.

The second formulation (Fig. 3) can be used if production data are unavailable on a per-well basis, though it is significantly less accurate, as it does not account for well operating efficiency. The first formulation is used throughout the remainder of this paper.

Error! Reference source not found. Fig. 4 illustrates the distribution of the first injectivity indicator for all available production wells on the NCS, highlighting values for reservoirs with the largest storage capacity. Predominantly gas reservoirs tend to exhibit significantly higher injectivity indicator scores than oil reservoirs. The correlation coefficient between the indicator and the gas share of HCPV is 0.61, which can be explained by the considerably lower viscosity of gas relative to oil. The distribution appears to follow a lognormal pattern, with the median around 2000 rm^3/day. At a CO_2 reservoir density of 650 kg/m^3, the median corresponds to approximately 1300 t/day or 0.47 Mt/year.

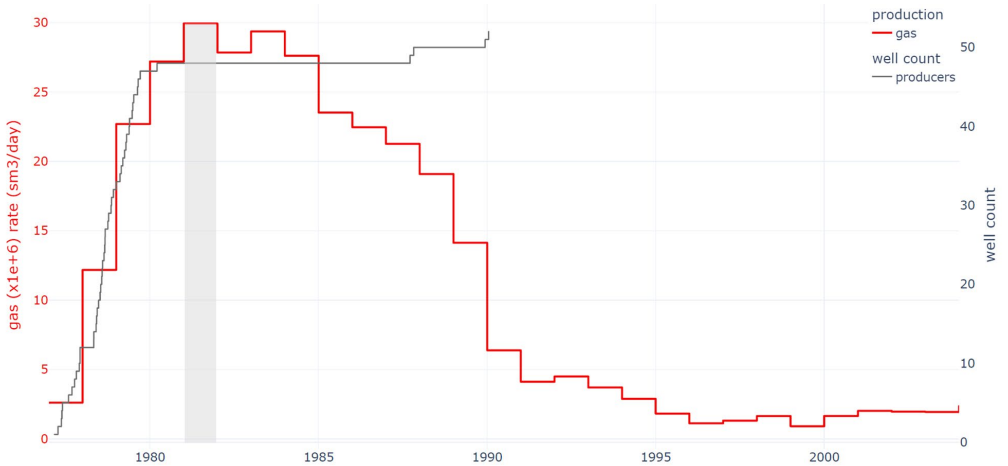

Fig. 3. Illustration of the second injectivity indicator: gas production rate (left y-axis) of the Frigg field and well count (right y-axis). The peak production year is shaded.

The injectivity indicator does not account for relative permeability effects, which are likely to be significant in multi-phase flow scenarios. However, it does account for viscosities of reservoir fluids and their flow properties, as if they were flowing ahead of the CO_2 plume at the initial pressure and temperature. The indicator does not account for advancements in drilling and completion technology, as wells completed in the 1990s and later are more likely to be horizontal or multilateral, and thus have higher productivity. Despite these limitations, we believe this approach provides reliable estimates suitable for screening purposes.

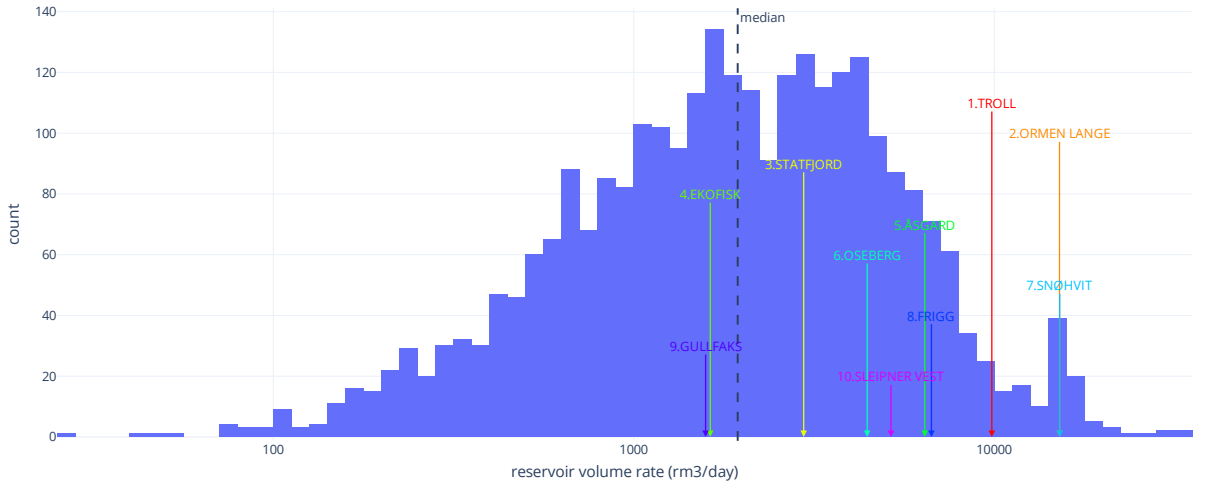

Fig. 4. Histogram of the decimal logarithm of the first injectivity indicator for all available production wells, with the top 10 fields by storage capacity marked. Tick values on the x-axis are exponentiated for readability.

Lifetime estimates. The following simple metrics are employed to characterize the extent of reserves depletion and expected abandonment time:

- **Maturity index**: the ratio of the current cumulative production to the original recoverable volume, ranging from 0 (no production) to 1 (completely depleted) for oil, gas, liquids, and oil equivalent (OE).
- **Remaining production years,** or **reserve lifetime**: the ratio of the remaining reserves to the current production of oil, gas, and oil equivalent (OE), applicable only to fields with a maturity index greater than 0.75.

These depletion metrics are simplistic and have many limitations. The maturity index may not be very informative, as a large field with a maturity index of 90% may produce much longer than a smaller green field. The reserve lifetime is applicable only to mature fields and represents a minimal remaining production time, as tail-end production rates tend to decline rather than remain constant. Therefore, it is likely to underestimate the remaining production time. To address these limitations, we incorporated additional data to improve the estimate of **remaining lifetime** of fields, including those with limited production history.

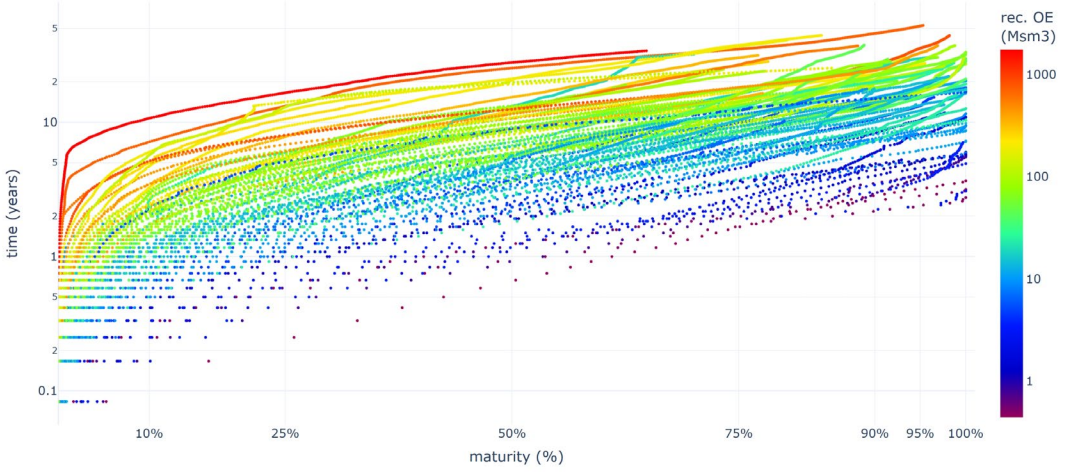

Fig. 5. Production time (years in log) vs. maturity of fields (%) on the NCS, colors reflect initial recoverable OE volumes.

Although production profiles vary significantly across fields due to many factors (Fig. 5), total lifetime shows a strong correlation with initial recoverable reserves. As illustrated in Fig. 6 (based on data from 30 shut-down fields and published estimates for Troll, Statfjord, and Ula), knowing only a field's recoverable OE volume $\boldsymbol{r}$ (Msm^3) enables a reasonable estimate of its total lifetime $\boldsymbol{t_{100}}$ (years):

$$log_{10}t_{100} = 0.393\ log_{10}r + 0.662$$

While this relationship explains approximately 83% of the variance on a log-log scale, the remaining 17% entails considerable uncertainty, which can be further reduced by incorporating available production data. For this purpose, we propose two methods.

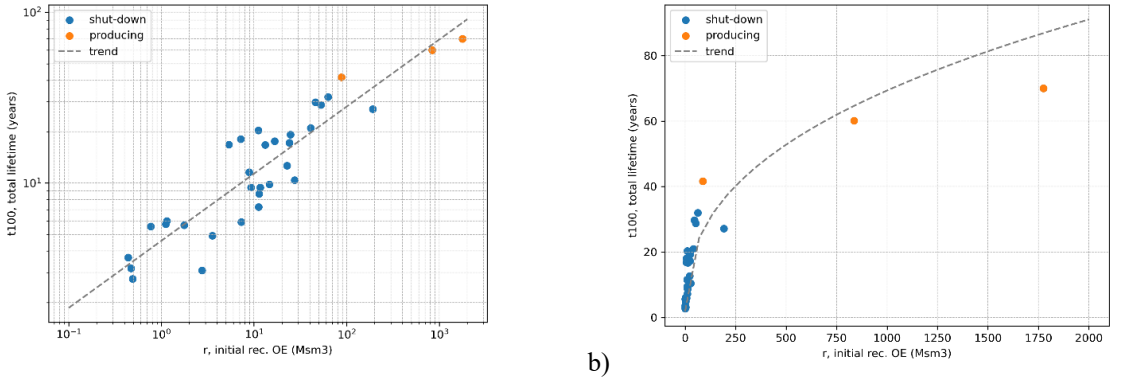

Fig. 6. Observed total lifetimes of the shut-down fields on the NCS (blue) and the estimates for a few producing (Troll, Statfjord, Ula – orange) vs. initial recoverable OE volume on (a) log-log, (b) linear scale. Recoverable volumes of cross-border fields are adjusted to the total values.

The first approach employs a regression model of remaining lifetime vs. recoverable oil equivalent and current production time. For each producing field with at least 10% maturity, a linear regression model is fit to data for shut-down fields: recoverable volumes and production times at the current maturity of the field in question. Otherwise, if not enough production history is available, the remaining lifetime is estimated from the initial recoverable reserves by means of the volumetric relationship above. While in-place volumes and production times are correlated, they do not completely overlap, as the latter factors in observed production dynamics.

The second, more sophisticated, method utilizes all observed production profiles on the NCS. Its core idea is to estimate the field's future production rates using its initial recoverable OE volume r, preceding production $\boldsymbol{q_{i-1}}$, and similarly, reserves $\boldsymbol{R}$ and historical rates $\boldsymbol{Q}$ of other fields. In more detail, the workflow is:

1. Divide all production profiles into N segments with equal maturities with a step Δm.
2. Iterate through the maturity segments. For the segment i:
   2.1. if the field produced during this segment => skip to the next one.
   2.2. else:
      if i = 1:
         fit a linear model $F(log_{10}R)$ to $log_{10}Q_i$
         calculate $log_{10}q_i = F(log_{10}r)$
      else:
         fit a linear model $F(log_{10}R, log_{10}Q_{i-1})$ to $log_{10}Q_i$
         calculate $log_{10}q_i = F(log_{10}r, log_{10}q_{i-1})$
   2.3. calculate the duration of the segment as $\Delta t_i = \Delta m r / q_i$

Thus, the described algorithm recursively estimates the production profile, accounting for available information from both the field in question and production history of other fields. Fig. 7 provides an example using the Frigg field, where the production profile is forecast from different points in its history.

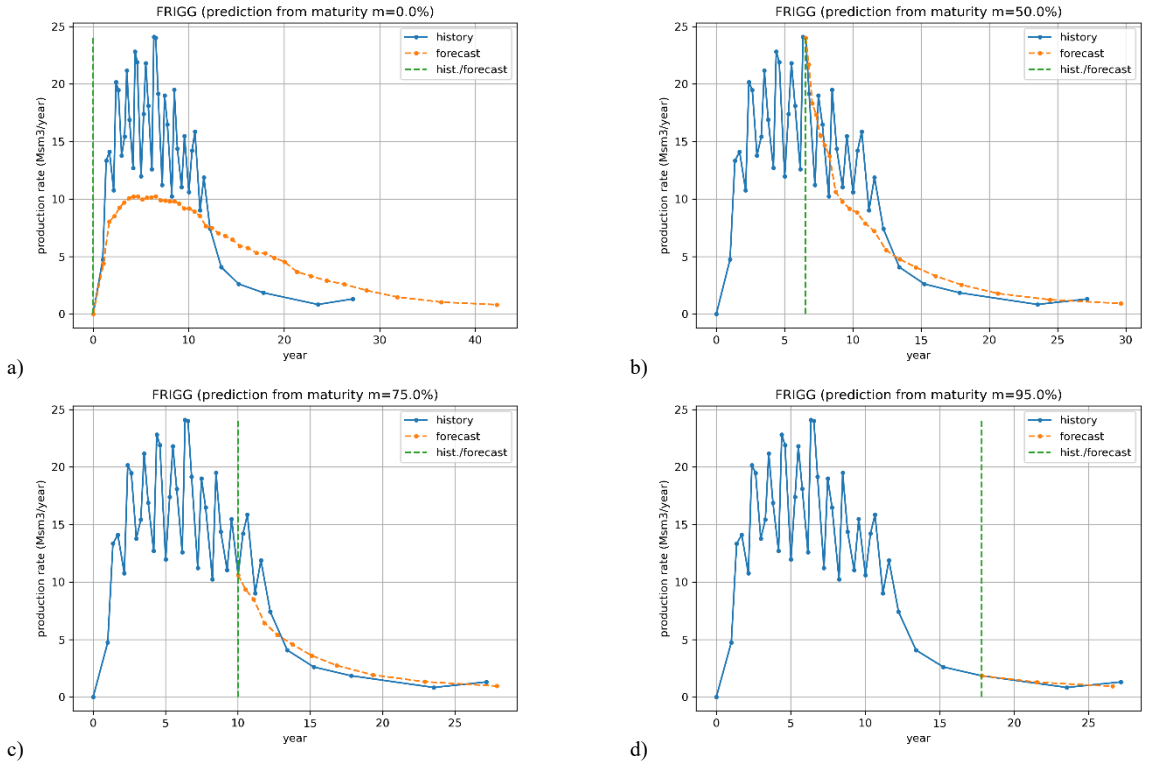

Fig. 7. Example of production profiles projected from different points of Frigg's production history.

Both methods have been tested as follows: remaining lifetimes of all abandoned fields were forecast from different maturities and compared with observed values. The resulting coefficients of determination, for both linear and logarithmic scales, are presented in Fig. 8. In our view, the logarithmic scale is more relevant due to 1) consistency with the data and their logarithmic transformations; 2) balanced weighting across field sizes; and 3) improved visibility of relative errors. The second method significantly outperforms the first on the logarithmic scale and achieves at least comparable accuracy on the linear one, except at the very beginning of production. Therefore, the second method is adopted for fields with a maturity of 10% or greater, and the volumetric relationship is used for greener fields.

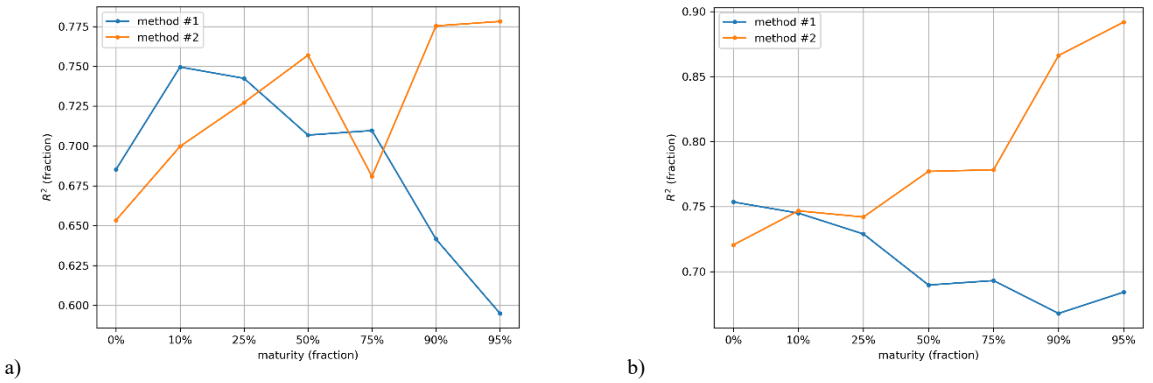

Fig. 8. R^2 of the methods for test results in (a) linear and (b) logarithmic scales. Note that the first point of the first method (at 0%) corresponds to the volumetric estimate.

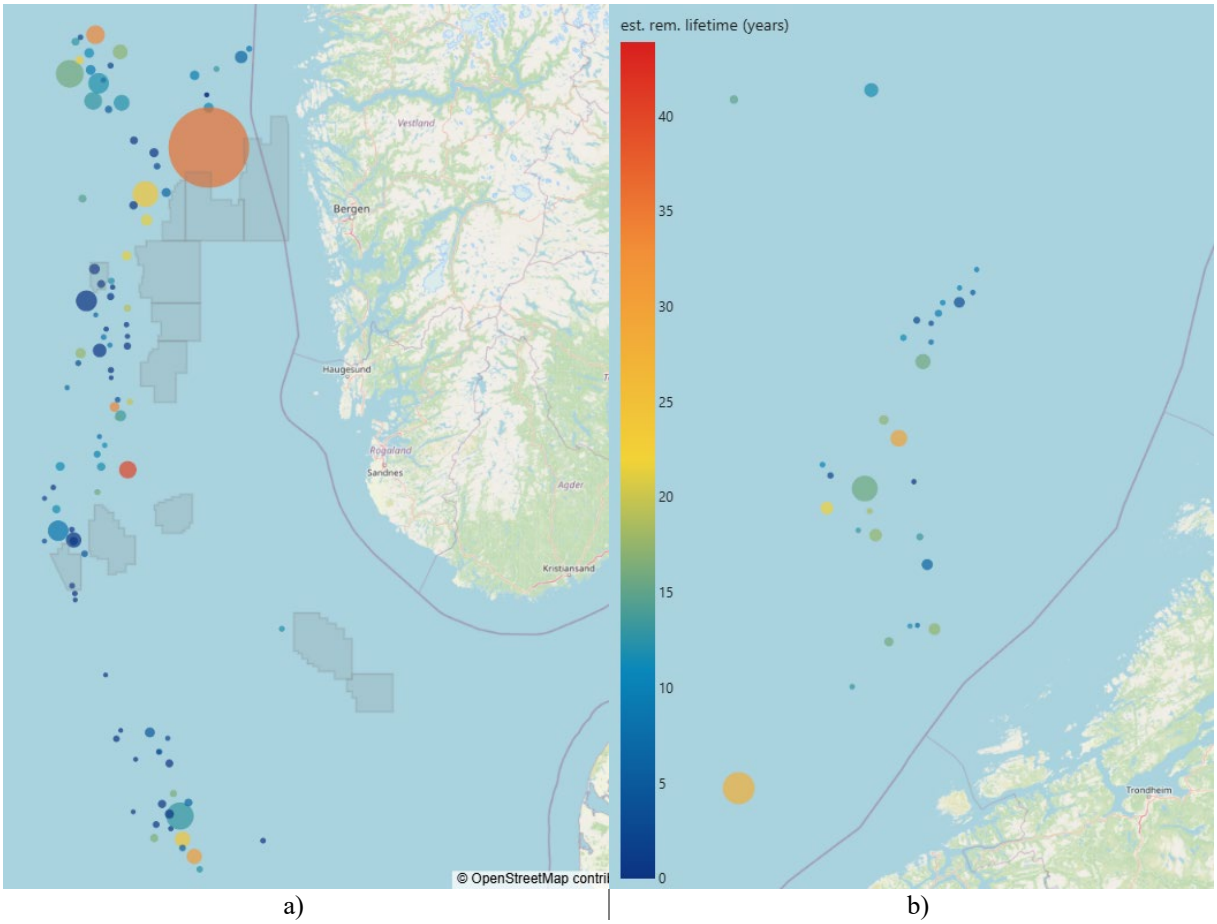

Fig. 9. (a) Fields in the Norwegian North Sea and (b) in the Norwegian Sea. Circle sizes and colors represent the CO2 storage indicator and the estimated remaining production time, respectively. Active CO_2 storage exploration and exploitation licenses are shaded.

2.3. Total score

The indicators described above, along with other parameters, have been compiled into a database that covers 134 Norwegian fields that have ever been approved for production. These indicators and other quantitative parameters can be aggregated into a **total score** – a single metric that characterizes a field's suitability for CO_2 storage. In our current implementation, the total score is calculated as a weighted average of normalized indicators as follows:

1) The user defines the parameters of interest and assigns them weights.
2) If a parameter needs to be minimized (e.g., remaining reserve lifetime before the reservoir can be converted to a CO_2 storage), it is transformed as follows:
   $x \rightarrow max(x) + min(x) - x$. This transformation ensures that components of the total score remain positive, primarily for visualization purposes. In the screening application described further, the user can indicate that a parameter needs to be minimized by assigning a negative weight.
3) A **utility function** is applied to each indicator to map its nominal value to a value meaningful to the user. For instance, if the utility function of the injectivity is $\log_{10}$, the increase from 1 to 10 sm^3/day/bar would result in the same increment of the utility function as the increase from 10 to 100 sm^3/day/bar. This step is optional.
4) The vectors are **normalized** using one (or two compatible) of the following methods:

a) the min-max scaling (default option) maps the parameter between 0 (worst) and 1 (best);
b) Z-score scaling centers the data around zero mean, with unit standard deviation;
c) median and mean scaling centers the data around 1 using median/mean value, respectively.

5) The **total score** is calculated as a weighted average of parameters based on user-defined weights, and the result is multiplied by 100.

The scoring procedure and data have been implemented in a web application for visualization and screening at *https://subcset-35e143428f88.herokuapp.com/*. Illustrative case studies are provided in the next section.

3. Demonstration of the screening tool

Since 1971, 134 fields on the NCS have been approved for oil and gas production. Fig. 9**Error! Reference source not found.** shows a map generated by the screening tool displaying all the fields with circle sizes and colors representing the storage capacity and injectivity indicators, respectively. Table 1 lists the ten largest fields in terms of the storage capacity indicator. The calculated total storage capacity indicator from all fields is approximately 18 Gt, with 64% originating from the ten largest fields. Notably, the Troll field stands out significantly, accounting for approximately one-third of the total storage capacity indicator. Fig. 11 presents cumulative storage capacity indicator vs. time based on estimates of remaining lifetimes.

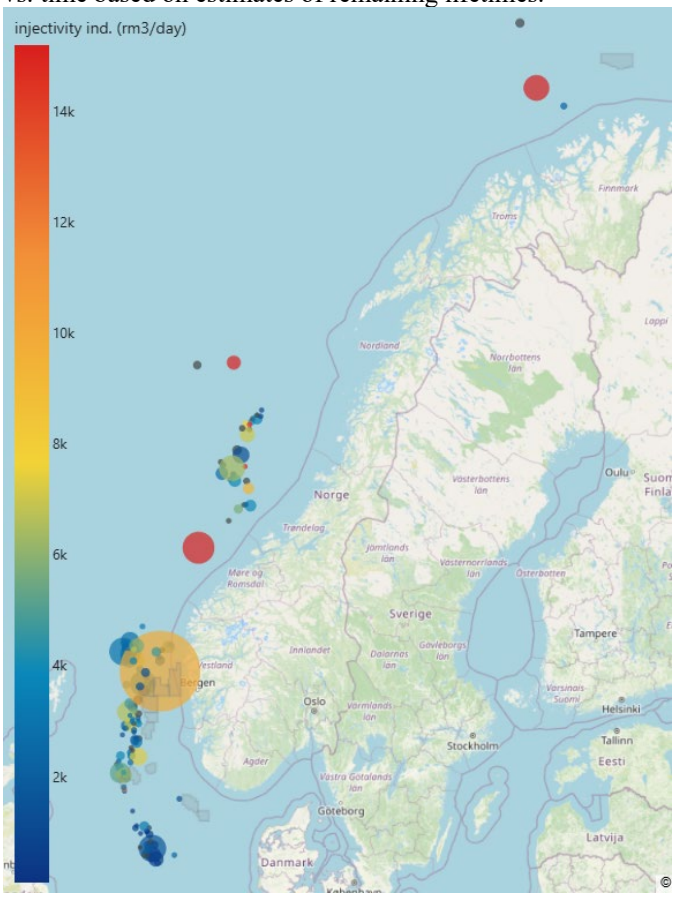

Fig. 10. Fields on the NCS, with circle size and color representing the storage capacity and injectivity indicators, respectively. Active CO_2 storage licenses are shaded.

#	field	HC type	maturity OE (fraction)	CO_2 SC indicator (Mt)
1	TROLL	gas/oil	0.648	6090.0
2	ORMEN LANGE	gas	0.776	972.0
3	STATFJORD	oil/gas	0.982	727.0
4	EKOFISK	oil	0.953	714.0
5	ÅSGARD	gas/oil	0.905	633.0
6	OSEBERG	oil/gas	0.881	632.0
7	SNØHVIT	gas	0.364	629.0
8	FRIGG	gas/oil	1	412.0
9	GULLFAKS	oil	0.969	399.0
10	SLEIPNER VEST	gas	0.955	396.0

Table 1. The largest fields by the storage capacity indicator. Note that the values for cross-border fields (Statfjord and Frigg) include only their Norwegian shares.

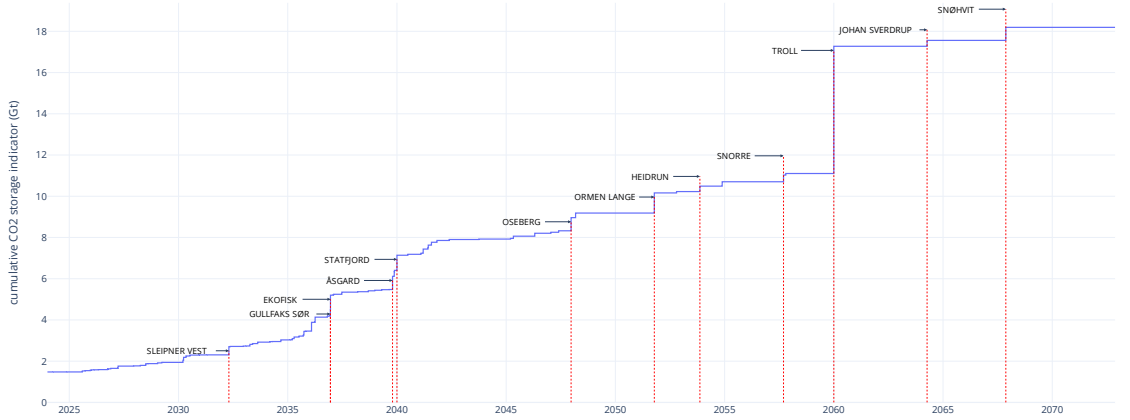

Fig. 11. Timeline of cumulative storage capacity indicator based on estimated field remaining lifetimes.

Fig. 12 displays a scatter plot of CO_2 density under initial reservoir conditions (y-axis) plotted against depth (x-axis), initial pressure gradient (marker color), and storage capacity indicator (marker size), with the largest fields labeled. Notably, the CO_2 density remains nearly constant at approximately 650 kg/m³ in fields under hydrostatic conditions (depicted in dark blue, forming a straight line along the bottom of the chart), almost independent of depth, as the effects of pressure and temperature offset each other.

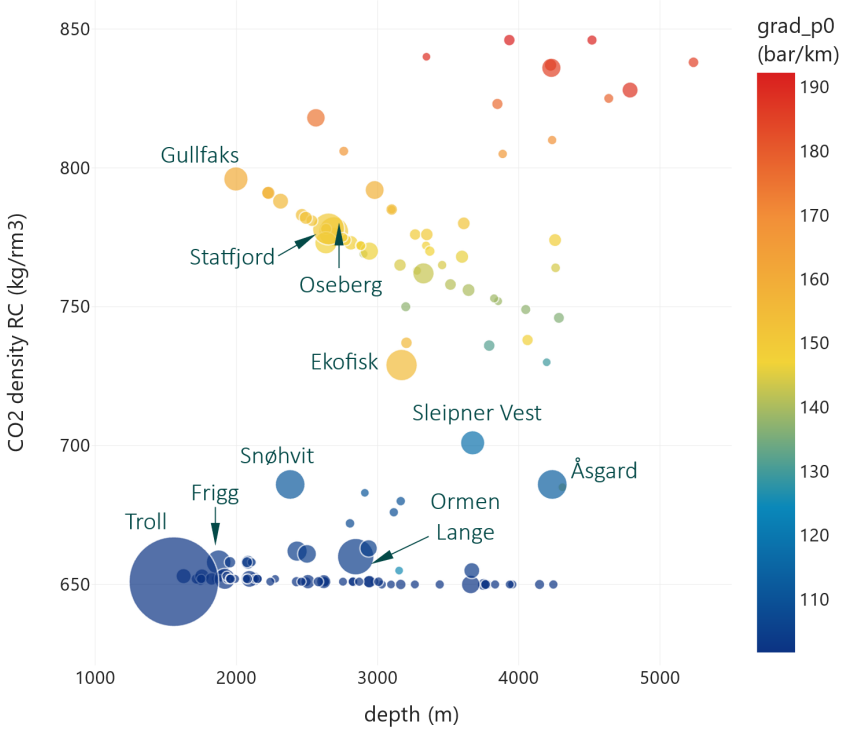

Fig. 12. All fields visualized: CO_2 density under initial reservoir conditions (y-axis) vs. depth (x-axis), with initial pressure gradient (marker color), and storage capacity indicator (marker size)

3.1. Case 1: Storing CO_2 close to available CCS infrastructure.

The first case illustrates how the screening tool can be used to evaluate storage candidates near available infrastructure. The ongoing Norwegian "Longship" full-scale CCS project will soon start injecting CO_2 in the Aurora area, under exploitation license EL001, southwest of the Troll field [10], [11]. The project's onshore facility in Øygarden (Western Norway) will serve as the receiving terminal for CO_2, which will be transported by pipeline to the Aurora offshore storage site. This area is particularly interesting because Aurora is bordered by the Smeaheia storage exploration license (ExL002) to the east and by the Luna exploration license (ExL004) to the west. Nine producing and two decommissioned fields are in immediate proximity to these licenses (Fig. 13).

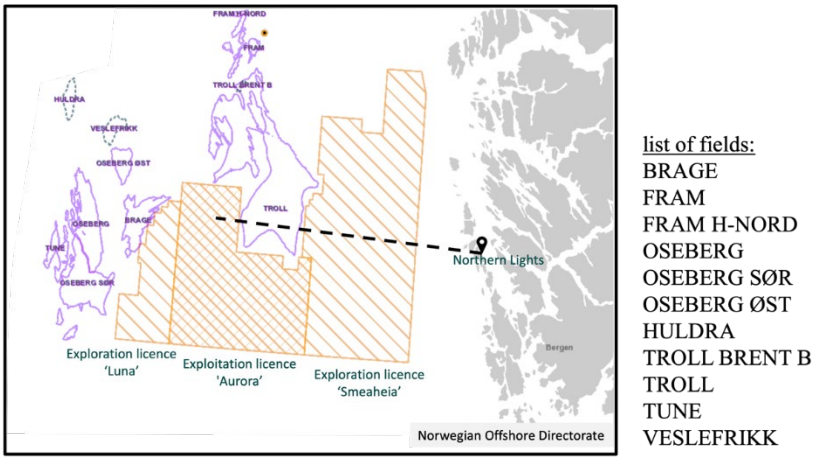

Fig. 13. Petroleum fields east and north of the Luna, Aurora, and Smeaheia licenses, west of the Northern Lights onshore facilities in Western Norway. The map was generated using FactMaps by the NOD (https://factmaps.sodir.no/factmaps).

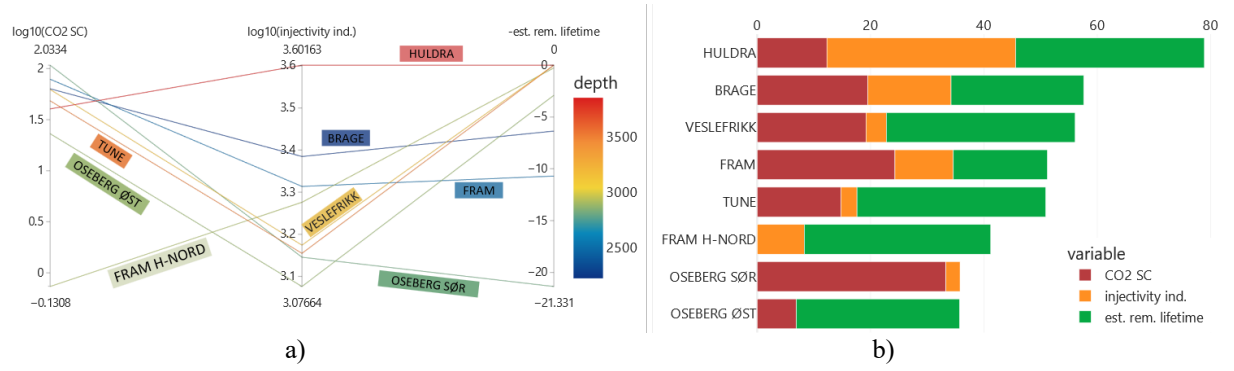

Fig. 14. (a) parallel plot of the storage capacity indicator, injectivity indicator, and estimated remaining lifetime, and depth (color) for the selected fields generated by the screening tool; (b) total score for the selected fields based on equal weights for the selected parameters.

After excluding Oseberg and Troll – large fields expected to remain in production for an extended period and serve as hubs for smaller fields – the remaining eight fields are evaluated using the indicators for capacity, injectivity, estimated remaining lifetime, and depth (Fig. 14a). The storage capacity, injectivity, and remaining lifetime indicators are selected to calculate the total score. These metrics are assigned equal weights and normalized using the min-max scaling. Based on ranking by the total score (Fig. 14**Error! Reference source not found.**b), we conclude that Huldra is the most suitable candidate, as it has high storage capacity, high injectivity, and is already abandoned (i.e., immediately available for CO_2 storage). However, it does not achieve the highest scores for all criteria, as its total score falls below 100.

3.2. Case 2: Storing CO_2 from a large emitter from petroleum activities nearby

Over the last 26 years, the Ekofisk field has been one of the largest emitters of CO_2 on the NCS, with an average emission of 0.76 Mt/year (0.53 Mt/year in 2023) [12]. In its vicinity, there are 14 mature and abandoned petroleum fields. Fig. 15 presents a map with these fields, where the size of each circle represents the storage capacity indicator (with Ekofisk displayed as the largest circle). Fig. 16a presents the storage capacity indicator, injectivity indicator, estimated remaining lifetimes, depth, and initial pressure gradient for these fields. Fig. 16b shows the fields ranked by the resulting total scores calculated with equal weights for the storage capacity, injectivity, and remaining lifetime indicators. In the described scenario, based on the total score, Ula, Vest Ekofisk, and Tommeliten Gamma are the best candidates to store CO_2 from Ekofisk. However, again, none of the fields is the best by all the criteria, as the highest total score, calculated using min-max scaling, falls below 100.

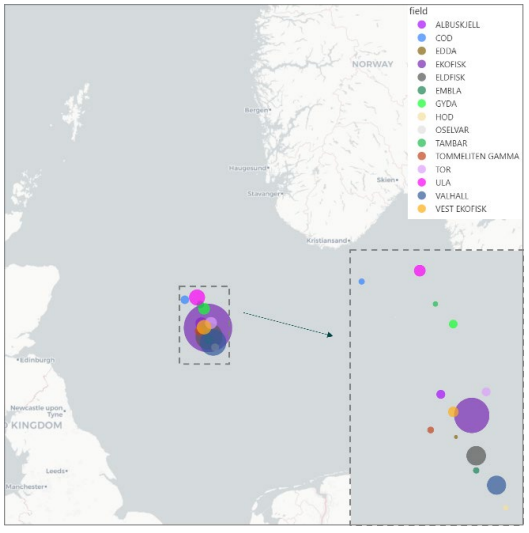

Fig. 15. Ekofisk and 14 mature or shut-down petroleum fields located nearby. The circle sizes reflect the storage capacity indicator.

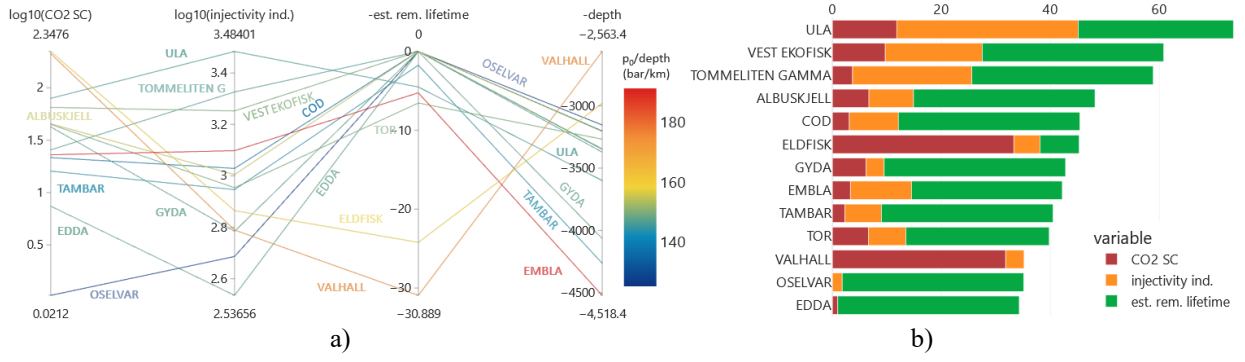

Fig. 16. (a) Parallel plot showing data for the selected neighboring fields of Ekofisk: storage capacity indicator, injectivity indicator, estimated remaining lifetime, depth, and initial pressure gradient (color); (b) total scores for these fields, calculated using equal weights for the selected parameters.

4. Discussion

We believe that the current study creates value by gathering, processing, enriching and analyzing public data, and redistributing the results back to the public domain. There remains considerable potential for further work in any of

these directions. The presented approach could be enhanced with more available data to provide a better and more nuanced assessment.

As briefly discussed above, the proposed approach is constrained by the data resolution and assumptions made to bridge missing data. In particular, this study is conducted in quasi-2D, as the data are aggregated at the field level and does not allow for discerning separate formations within a given field.

While introducing the indicators, we have already touched upon some of their limitations. The **storage capacity indicator** does not account for compaction, communication with adjacent aquifers, and water volumes injected for pressure support. Nor does this indicator account for sweep, displacement, and drainage efficiency factors of CO_2 storage, which are the subjects of detailed studies. We believe that integration of dynamic pressure measurements would allow for delineating compaction effects and aquifer communication. The same applies to water volumes injected. In the current study, we did not manage to integrate injected water volumes due to data availability and verification difficulties, though it would greatly enhance estimates for oil fields produced under waterflooding. The reduction of available pore volume due to water injection will decrease the storage capacity estimates, especially in confined reservoirs. However, this impact is not likely to be very significant for the total storage capacity as its bulk (69%) is associated with pore volumes released in gas fields, which are normally depleted without pressure support. Moreover, the current formulation of the storage capacity indicator does not account for possible upsides due to 1) additional capacity associated with adjacent aquifers and 2) pressurization above the initial pressure. The latter can be addressed by integrating fracturing pressure estimates from leak-off tests [13],[14].

In general, we are cautious about equating the storage capacity indicator with a bankable storage capacity, as the former has the limitations mentioned above, while the latter is subject to certain methodological vagueness that can hardly be resolved without detailed, case-by-case studies. Overall, the indicator falls into the category of static storage capacity estimates, which may significantly exceed commercial capacity. As hydrocarbons are trapped within deposits covered by caprocks, injected CO_2 is unlikely to migrate upwards, provided that there is no leakage through legacy wells or severe fracturing. Therefore, we believe that, in the first approximation, the entire released HCPV can be claimed for CO_2 storage. For comparison, previously Emmel et al. [19] estimated a theoretical storage capacity for the Norwegian part of the Frigg field in the range of 355–422 Mt, which encompasses our estimate of the storage capacity indicator at 416 Mt.

During CO_2 injection, three flow regions emerge: 1) CO_2 around the well, 2) CO_2 mixed with original fluids (brine, oil, gas), and 3) original fluids displaced away from the well by the CO_2 plume. The proposed **injectivity indicator** is based on production data and, hence, the most suitable to describe the third region. It reflects the flowing properties of original fluids but does not account for CO_2 and multiphase flow in the first and second regions. The injectivity indicator formulation could further be refined, for instance, through simple analytical models for solvent flooding and/or numerical modeling. Above, it was demonstrated (Fig. 4) that the injectivity indicators of individual wells on the NCS follow a pseudo-lognormal distribution, which may reflect fundamental laws governing the distribution of flow properties, such as permeability. At the field level, the distribution of historical well rates can be utilized to characterize heterogeneity and assess the uncertainty associated with injectivity.

The **reserve lifetime** indicator is quite simple, yet imprecise and applicable only to mature fields. The proposed more advanced, data-driven formulations are more accurate and have much broader applicability. However, they still depend on reserve estimates, which may increase (for instance, due to additional drilling or infrastructure upgrades) or be revised downward. Field investments reported by the NOD could serve as a forward-looking indicator and improve the accuracy of estimates.

Introducing an **energy efficiency indicator** would allow for ranking reservoirs by specific energy per CO_2 unit stored.

5. Summary and conclusions

This study utilizes publicly available data from nearly all Norwegian petroleum fields to assess their CO_2 storage potential using indicators for key parameters such as storage capacity, injectivity, maturity, and remaining lifetime. The total storage capacity indicator for the NCS was estimated at 18 Gt, with 64% attributed to the ten largest fields and 69% to gas production.

The presented approach stands out in its simplicity, transparency, reproducibility, and reliance solely on open data. The proposed methodology is not intended to provide a comprehensive analysis; however, it can still narrow the list of available options, answer essential questions, and highlight knowledge gaps to be addressed in detailed studies. Additionally, the findings and data from this study have broader applications, such as hydrogen storage, demonstrating significant potential for further reuse of data from petroleum reservoirs.

The repository with the data and codes is available at *https://github.com/cssr-tools/SubCSeT*. A web application for data visualization and screening can be accessed at *https://subcset-35e143428f88.herokuapp.com/*. We hope that open access to the data, codes, and screening application will encourage other researchers and stakeholders to build upon them.

6. Acknowledgement

The authors acknowledge funding from the Centre of Sustainable Subsurface Resources (CSSR), grant nr. 331841, supported by the Research Council of Norway, research partners NORCE Norwegian Research Centre and the University of Bergen, and user partners Equinor ASA, Harbour Energy Norge AS, Sumitomo Corporation, Earth Science Analytics, GCE Ocean Technology, and SLB Scandinavia.

Nomenclature

FVF	formation volume factor (rm^3/sm^3)
GOR	gas-oil ratio (sm^3/sm^3)
HCPV	hydrocarbon pore volume (rm^3)
NCS	Norwegian Continental Shelf
OE	oil equivalent (1 sm^3 of oil or 1000 sm^3 of natural gas)
PVT	pressure volume temperature (fluid properties)
SSTVD	subsea true vertical depth (m)

References

[1] Resource report 2024. Norwegian Offshore Directorate. [Internet], 2024, Available from: https://www.sodir.no/en/whats-new/publications/reports/resource-report/resource-report-2024/

[2] U.S. Department of Transportation. Fact Sheet: Underground Natural Gas Storage Caverns | PHMSA [Internet]. 2021, Available from: https://www.phmsa.dot.gov/technical-resources/pipeline/underground-natural-gas-storage/fact-sheet-underground-natural-gas

[3] FactPages. Norwegian Offshore Directorate [Internet], Available from: https://factpages.sodir.no/

[4] DISKOS database. Public production [Internet], Available from: www.diskos.com

[5] Khrulenko A. SubCSeT project repository [Internet], Available from: https://github.com/cssr-tools/SubCSeT

[6] Alnes H., Eiken O., Nooner S., Sasagawa G., Stenvold T., Zumberge M. Results from Sleipner gravity monitoring: Updated density and temperature distribution of the CO_2 plume. Energy Procedia. 2011;4:5504–11.

[7] Moss B., Barson D., Rakhit K., Dennis H., Swarbrick R. Formation pore pressures and formation waters. In: The Millennium Atlas: petroleum geology of the central and northern North Sea. Evans, D, Graham, C, Armour, A, and Bathurst, P (editors and co-ordinators). London: The Geological Society of London.; 2003. p. 317–29.

[8] Lemmon E.W., Bell I.H., Huber M.L., McLinden M.O.. Thermophysical Properties of Fluid Systems in NIST Chemistry WebBook. NIST Standard Reference Database Number 69, Eds. P.J. Linstrom and W.G. Mallard, National Institute of Standards and Technology, Gaithersburg MD, 20899, [Internet]. Available from: https://doi.org/10.18434/T4D303

[9] Ramírez A., Hagedoorn S., Kramers L., Wildenborg T., Hendriks C. Screening CO_2 storage options in The Netherlands. International Journal of Greenhouse Gas Control. 2010 Mar;4(2):367–80.

[10] Ministry of Petroleum and Energy. Longship – Carbon capture and storage — Meld. St. 33 (2019–2020) Report to the Storting (white paper) [Internet]. 2020. Available from: https://www.regjeringen.no/en/dokumenter/meld.-st.-33-20192020/id2765361/
[11] Equinor. Northern Lights FEED report [Internet]. Available from: https://norlights.com/wp-content/uploads/2021/03/Northern-Lights-FEED-report-public-version.pdf
[12] The Norwegian Environment Agency. Ekofisk: Releases of Carbon dioxide (CO_2) [Internet]. Available from: https://www.norskeutslipp.no/en/Miscellaneous/Company/?CompanyID=22344&ComponentPageID=1162
[13] Gaarenstroom L., Tromp R.A.J., De Jong M.C., Brandenburg A.M. Overpressures in the Central North Sea: implications for trap integrity and drilling safety. PGC. 1993 Jan;4(1):1305–13.
[14] Nordgård Bolås H.M., Hermanrud C. Hydrocarbon leakage processes and trap retention capacities offshore Norway. PG. 2003 Oct;9(4):321–32.
[15] Norwegian Petroleum Directorate. CO_2 atlas for the Norwegian Continental Shelf [Internet]. 2014. Available from: https://www.sodir.no/en/whats-new/publications/co2-atlases/co2-atlas-for-the-norwegian-continental-shelf/
[16] Bachu S. Identification of oil reservoirs suitable for CO2 -EOR and CO2 storage (CCUS) using reserves databases, with application to Alberta, Canada. International Journal of Greenhouse Gas Control. 2016 Jan;44:152–65.
[17] Bergmo P.E.S., Emmel B.U., Anthonsen K.L., Aagaard P., Mortensen G.M., Sundal A. Quality Ranking of the Best CO_2 Storage Aquifers in the Nordic Countries. Energy Procedia. 2017 Jul;114:4374–81.
[18] IEAGHG, "Criteria for Depleted Reservoirs to be Developed for CO_2 Storage ", 2022-01, January 2022. Available from: https://ieaghg.org/publications/criteria-for-depleted-reservoirs-to-be-developed-for-co2-storage/
[19] Emmel B, Romdhane A, Dupuy B, Zonetti S, Barrabino A. De-risking legacy well integrity to unlock storage potential of the Frigg field, North Sea Norway. In European Association of Geoscientists & Engineers; 2023 [cited 2025 May 28]. p. 1–5. Available from: https://www.earthdoc.org/content/papers/10.3997/2214-4609.202310753